Neuromechanical Simulation of Human Postural Sway in the Sagittal Plane Based on a Hybrid Triple Inverted Pendulum Model and State-Dependent Intermittent Neural Control

Yongkun Zhao†, *Member, IEEE*, Mingquan Zhang†, *Member, IEEE*, Balint K. Hodossy, Jiatong Jiang, Masahiro Todoh, *Member, IEEE*, and Dario Farina*, *Fellow, IEEE*

***Abstract*— This study introduces a novel neuromechanical model that employs a hybrid triple inverted pendulum (HTIP) framework combined with state-dependent intermittent control to simulate human quiet stance in the sagittal plane. Our model integrates the biomechanics of the ankle, knee, and hip joints, focusing on the stabilization of the body's center of mass (CoM) rather than controlling each joint individually. Unlike computational models that require precise joint control, the central nervous system maintains posture by simplifying neural control mechanisms. Specifically, the state-dependent control strategy activates neural feedback only as the CoM approaches the stability boundaries. Our HTIP model includes these physiological mechanisms, providing a computationally efficient mechanism for posture control. Experimental validation against real-world data demonstrated that our model can accurately replicate natural postural sway patterns in the sagittal plane, addressing a long-standing challenge in neuromechanical modeling of human quiet standing. This enhanced understanding and simulation capability offers significant new insights for developing targeted interventions for individuals with impairments in postural control.**

***Index Terms*— Neuromechanical modeling, human quiet stance, center of mass stabilization, intermittent control, natural postural sway.**

I. Introduction

CURRENTLY, many countries around the world are facing the severe challenge of an aging population [1]. Falls among the elderly can lead to fatal injuries or long-term mobility issues, presenting a significant socio-economic challenge to society [2]. To effectively predict and prevent falls, a comprehensive understanding of the neural control mechanisms behind human quiet stance posture in the sagittal plane is crucial, as it forms the basis for various bipedal activities in daily life [3]. Maintaining a quiet stance posture is a fundamental yet extremely complex task, involving intricate neuromechanical interactions [4], [5]. Despite extensive research, accurately simulating the dynamic balance and natural postural sway observed in humans remains a challenge, necessitating the development of new neuromechanical models [6], [7].

Neuromechanical modeling primarily consists of two parts: the human body model and the neural feedback control mechanism [8]. Traditional neuromechanical models for human quiet stance have widely adopted single inverted pendulum (SIP) and double inverted pendulum (DIP) descriptions, providing valuable insights into the biomechanical processes of quiet stance [9]–[14]. However, these models often simplify human body structure and overlook important joints, such as the knee joint [15]. The SIP model only involves the ankle joint [16], while the DIP model considers both the ankle and hip joints [17]. This simplification fails to account for the natural sway of the knee joint and its significant coordination with the hip and ankle joints in quiet stance [18]–[20].

At the same time, the neural feedback control mechanism for human quiet stance remains a subject of considerable debate [21]–[23]. So far, various conceptual neural feedback control models have been proposed to explain the basis of human quiet posture maintenance [24]–[28]. One prominent model is the continuous impedance control model, which effectively combines the physiological characteristics of human body stiffness and damping through the mathematical expression of proportional (P) and derivative (D) feedback gains [24], [29]. However, due to the inherent delay in neural signal transmission, continuous control models cannot maintain body balance effectively, potentially leading to system instability [30]–[32]. Moreover, experimental studies have shown that muscle activity during quiet stance is not continuous but exhibits intermittent activation characteristics [22], [33]. Con-

This work was supported by the Japan Society for the Promotion of Science (JSPS) KAKENHI for Research Fellowships for Young Scientists, Grant Number 24KJ0280, and in part by the Japan Science and Technology Agency (JST) for Support for Pioneering Research Initiated by the Next Generation (SPRING), Grant Number JPMJSP2119.

First authors: Yongkun Zhao and Mingquan Zhang; Corresponding author: Dario Farina.

Yongkun Zhao, Balint K. Hodossy, Jiatong Jiang, and Dario Farina are with the Department of Bioengineering, Faculty of Engineering, Imperial College London, London SW7 2AZ, United Kingdom (email: y.zhao22@imperial.ac.uk; balint.hodossy16@imperial.ac.uk; jiatong.jiang@imperial.ac.uk; d.farina@imperial.ac.uk)

Mingquan Zhang is with the Division of Human Mechanical Systems and Design, Graduate School of Engineering, Hokkaido University, Sapporo 060-8628, Japan (mingquan.zhang@ieee.org).

Masahiro Todoh is with the Division of Mechanical and Aerospace Engineering, Faculty of Engineering, Hokkaido University, Sapporo 060-8628, Japan (todoh@eng.hokudai.ac.jp).

sequently, several intermittent neural control models based on time and state have been proposed. In time-based models, the neural controller periodically receives postural position feedback and calculates the appropriate neural feedback torque based on the human body model [34], [35]. However, this approach heavily relies on the accuracy of the body model, which does not align with how the central nervous system (CNS) controls standing posture; the CNS cannot perceive complex human body models and cannot perform precise torque calculations [36]–[38]. Furthermore, the simulation results of this type of intermittent control theory have not demonstrated the natural postural sway observed in human quiet stance [39], [40]. State-based intermittent control models offer a more likely explanation, where the brain only provides neural feedback torque to maintain an upright posture when the body's center of mass (CoM) deviates significantly [41]–[44]. Nonetheless, this assumption also faces challenges, especially when the human body model includes multiple joints that would require the neural controller to calculate the appropriate neural feedback torques for several joints separately [17]. This is also computationally demanding. More importantly, the primary goal during quiet stance is to stabilize the human body's CoM, not to control each joint individually [15], [45], [46].

In this study, we propose a novel neuromechanical model that integrates a hybrid triple inverted pendulum (HTIP) model with a state-dependent intermittent control strategy, aiming to more accurately simulate the human quiet stance state than currently possible. The main contributions of our work are summarized as follows:

- **Development of the HTIP model:** Our research contributes to the field by developing a comprehensive model that incorporates the dynamics of the ankle, knee, and hip joints along with the corresponding lower leg, upper leg, and torso segments. This model overcomes the limitations of traditional neuromechanical models that predominantly use simplified single or double inverted pendulum models, thus providing a simulation of human quiet stance that more closely approximates real-world dynamics. The HTIP framework effectively combines a triple inverted pendulum (TIP) model with a virtual single inverted pendulum (VSIP) model, simplifying the computational process while maintaining the complexity necessary to accurately represent human anatomy and postural mechanics in the sagittal plane.
- **State-dependent intermittent control:** By adopting a state-dependent intermittent control strategy, our model activates neural feedback only when the body's motion state approaches unstable boundaries. This approach is grounded in physiological observations that suggest human neural control operates intermittently, rather than continuously. This aligns with the natural postural adjustments observed in quiet human standing. This intermittent control model offers a plausible explanation for how the human CNS manages the complex dynamics of multi-joint control and motion stability with limited computational demand.
- **Simulation of natural postural sways:** The integration of HTIP with state-dependent intermittent control allows for more accurate simulations of natural postural sways in the sagittal plane. This advancement addresses a longstanding challenge in neuromechanical modeling of human quiet stance, as it enables the simulation to reflect the nuanced real-world movements observed in human balance maintenance. By improving the fidelity of the model against experimental data and validating it with motion capture results, our study not only enhances the understanding of human postural dynamics but also sets a new benchmark for the simulation of quiet stance that can be particularly useful in designing interventions for individuals with postural control impairments.

The remainder of the paper is structured as follows: Section II details the methodology of this study, divided into two main parts: one employing a HTIP model to represent the human body in the sagittal plane, and the other depicting the complex neuromechanical interactions involved in human quiet stance posture through a state-dependent intermittent control strategy. Both components are grounded in neuromechanical principles and articulated through computable mathematical formulas, enabling us to simulate the CoM and natural postural sway of various joints in the sagittal plane during human quiet stance. Section III presents these simulation results and compares them with joint and CoM sway data obtained through motion capture technology, thereby validating the reliability of the proposed neuromechanical model. Section IV discusses the significance of our research findings, elucidating the innovation of the study and its contributions to the field. This section also compares and discusses the simulation results with experimental results, further verifying the model's reliability. It also outlines the study's limitations and proposes directions for future research, especially regarding the refinement of the model. Section V concludes our study, summarizing our methodology and results, and reiterating the importance of our novel modeling approach and its potential in enhancing the understanding and simulation of human postural stability. The appendices provide detailed mathematical derivations of the HTIP model, supporting the computational framework and findings presented in the article.

II. Methods

A. Human Body Model

We propose a new approach based on the HTIP model to represent human body during quiet stance. This study is dedicated to contributing a comprehensive model to the field of neuromechanical modeling to capture the complex dynamics of human quiet stance in the sagittal plane. Unlike traditional methods, our model integrates a TIP model with a VSIP model to reduce the computational load. The TIP model precisely simulates the dynamics of the ankle, knee, and hip joints, along with the corresponding lower leg, upper leg, and torso segments, while the VSIP model represents the overall model dynamics in a simplified form. The CoM in the VSIP model is not based on any single part but represents the entire TIP model's CoM. This design allows

us to simplify the calculation based on the overall model's CoM position, determining the appropriate torque needed to maintain overall balance. Through this method, we not only reduce the computational load but also more comprehensively simulate the interaction between the lower limbs and torso and their impact on human balance. This new approach is also closer to the actual mechanisms of human posture adjustment since the CNS relies on the perception of the overall CoM displacement to adjust and control.

1) TIP Model: The physically simulated element of the HTIP model in the sagittal plane consists of three joints and three links, representing the human body's ankle, knee, and hip joints, as well as the segments of the lower leg (shank), upper leg (thigh), and the torso (trunk). The range of motion for each joint is specified as constraints for the simulation, with the mass, length, and the distance from the bottom of each segment to its CoM detailed for each link. The parameters are sequentially labeled from bottom to top, with the joints labeled as ankle, knee, and hip (1-3), and the segments as shank, thigh, and trunk (1-3). The framework of TIP model is shown in Fig. 1.

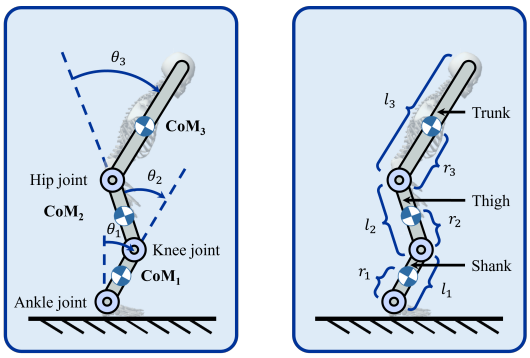

i (Segment index)	1 (Shank)	2 (Thigh)	3 (Trunk)
m_i (Segment mass)	6.478 kg	15.059 kg	51.6481 kg
l_i (Segment length)	0.431 m	0.430 m	0.715 m
I_i (Segment moment of inertia)	0.122 kg·m^2	0.291 kg·m^2	3.012 kg·m^2
r_i (Distance from the distal end of segment to its CoM)	0.245 m	0.244 m	0.356 m

Fig. 1. TIP model framework in the sagittal plane and simulation parameters [47].

The dynamic equations of TIP model are derived using the Lagrangian mechanics approach, which is particularly suited for analyzing the motion of multi-segmented systems subject to constraints.

The detailed dynamic equations of the TIP model are described as follows:

$$\mathbf{M}(\boldsymbol{\theta})\ddot{\boldsymbol{\theta}} + \mathbf{C}(\boldsymbol{\theta},\dot{\boldsymbol{\theta}})\dot{\boldsymbol{\theta}} + \mathbf{G}(\boldsymbol{\theta}) = \boldsymbol{\tau}(t) \tag{1}$$

where $\boldsymbol{\theta}$ represents the vector of joint angles in the sagittal plane, indicating the positions of the respective segments: shank, thigh, trunk, relative to each other. $\dot{\boldsymbol{\theta}}$ is the vector of angular velocities, which indicates how quickly the joint angles $\boldsymbol{\theta}$ are changing over time. $\ddot{\boldsymbol{\theta}}$ is the vector of angular accelerations, which represents how quickly the angular velocities $\dot{\boldsymbol{\theta}}$ themselves are changing over time. $\mathbf{M}(\boldsymbol{\theta})$ represents the mass matrix of the TIP model, which is influenced by $\boldsymbol{\theta}$. $\mathbf{C}(\boldsymbol{\theta},\dot{\boldsymbol{\theta}})$ symbolizes the Coriolis and centrifugal forces within the system. These forces are crucial for modeling the internal forces that arise from the movement of the body's segments during postural sway, affecting the overall stability. $\mathbf{G}(\boldsymbol{\theta})$ is the gravitational force matrix. It plays a vital role in postural stability by representing how gravity acts on the different segments of the body, depending on their orientation and position. $\boldsymbol{\tau}$ is the vector of torques at the joints, which can be interpreted as the neural control inputs necessary to counteract perturbations and maintain posture. This includes the neural feedback torques applied by the body to stabilize the CoM during quiet stance and counteract gravity, as well as any external perturbations the system might encounter. The detailed equations of these three matrices are as follows:

First, the element M_{ij} of matrix $\mathbf{M}(\boldsymbol{\theta})$ is described below:

$$\begin{aligned} M_{11} = {} & I_1 + I_2 + I_3 + l_1^2 m_2 + l_1^2 m_3 + l_2^2 m_3 \\ & + m_1 r_1^2 + m_2 r_2^2 + m_3 r_3^2 + 2 l_1 m_3 r_3 c_{23} \\ & + 2 l_1 l_2 m_3 c_2 + 2 l_1 m_2 r_2 c_2 + 2 l_2 m_3 r_3 c_3 \end{aligned} \tag{2}$$

$$\begin{aligned} M_{12} = M_{21} = {} & I_2 + I_3 + l_2^2 m_3 + 2 l_2 m_3 r_3 c_3 \\ & + l_1 l_2 m_3 c_2 + m_2 r_2^2 + l_1 m_2 r_2 c_2 \\ & + m_3 r_3^2 + l_1 m_3 r_3 c_{23} \end{aligned} \tag{3}$$

$$M_{13} = M_{31} = I_3 + m_3 r_3^2 + l_1 m_3 r_3 c_{23} + l_2 m_3 r_3 c_3 \tag{4}$$

$$\begin{aligned} M_{22} = {} & I_2 + I_3 + m_3 l_2^2 + 2 l_2 m_3 r_3 c_3 + m_2 r_2^2 \\ & + m_3 r_3^2 \end{aligned} \tag{5}$$

$$M_{23} = M_{32} = I_3 + m_3 r_3^2 + l_2 m_3 r_3 c_3 \tag{6}$$

$$M_{33} = I_3 + m_3 r_3^2 \tag{7}$$

Second, the element C_{ij} of matrix $\mathbf{C}(\boldsymbol{\theta})$ is described below:

$$\begin{aligned} C_{11} = {} & -\left(l_1 m_2 r_2 s_2 + l_1 m_3 r_3 s_{23} + l_1 l_2 m_3 s_2\right)\dot{\theta}_2 \\ & -\left(l_2 m_3 r_3 s_3 + l_1 m_3 r_3 s_{23}\right)\dot{\theta}_3 \end{aligned} \tag{8}$$

$$\begin{aligned} C_{12} = {} & -\left(l_1 m_2 r_2 s_2 + l_1 m_3 r_3 s_{23} + l_1 l_2 m_3 s_2\right)\dot{\theta}_1 \\ & -\left(l_1 m_2 r_2 s_2 + l_1 m_3 r_3 s_{23} + l_1 l_2 m_3 s_2\right)\dot{\theta}_2 \\ & - m_3 r_3 \left(l_2 s_3 + l_1 s_{23}\right)\dot{\theta}_3 \end{aligned} \tag{9}$$

$$\begin{aligned} C_{13} = {} & - m_3 r_3 \left(l_2 s_3 + l_1 s_{23}\right)\dot{\theta}_1 \\ & - m_3 r_3 \left(l_2 s_3 + l_1 s_{23}\right)\dot{\theta}_2 \\ & - m_3 r_3 \left(l_2 s_3 + l_1 s_{23}\right)\dot{\theta}_3 \end{aligned} \tag{10}$$

$$\begin{aligned} C_{21} = {} & \left(l_1 m_2 r_2 s_2 + l_1 m_3 r_3 s_{23} + l_1 l_2 m_3 s_2\right)\dot{\theta}_1 \\ & - l_2 m_3 r_3 s_3 \dot{\theta}_3 \end{aligned} \tag{11}$$

$$C_{22} = - l_2 m_3 r_3 s_3 \dot{\theta}_3 \tag{12}$$

$$C_{23} = - l_2 m_3 r_3 s_3 \dot{\theta}_1 - l_2 m_3 r_3 s_3 \dot{\theta}_2 - l_2 m_3 r_3 s_3 \dot{\theta}_3 \tag{13}$$

$$C_{31} = \left(l_2 m_3 r_3 s_3 + l_1 m_3 r_3 s_{23}\right)\dot{\theta}_1 + l_2 m_3 r_3 s_3 \dot{\theta}_2 \tag{14}$$

$$C_{32} = l_2 m_3 r_3 s_3 \dot{\theta}_1 + l_2 m_3 r_3 s_3 \dot{\theta}_2 \tag{15}$$

$$C_{33} = 0 \tag{16}$$

Third, the element G_i of matrix $\mathbf{G}(\boldsymbol{\theta})$ is described below:

$$G_1 = -g((l_1 m_2 + l_1 m_3 + m_1 r_1)s_1 + (l_2 m_3 + m_2 r_2)s_{12} + m_3 r_3 s_{123}) \quad (17)$$

$$G_2 = -g((l_2 m_3 + m_2 r_2)s_{12} + m_3 r_3 s_{123}) \quad (18)$$

$$G_3 = -g m_3 r_3 s_{123} \quad (19)$$

where c_2 denotes $\cos(\theta_2)$, c_3 denotes $\cos(\theta_3)$, and c_{23} denotes $\cos(\theta_2 + \theta_3)$. Similarly, s_1 represents $\sin(\theta_1)$, s_2 represents $\sin(\theta_2)$, s_3 represents $\sin(\theta_3)$, s_{12} represents $\sin(\theta_1 + \theta_2)$, s_{23} represents $\sin(\theta_2 + \theta_3)$, and s_{123} represents $\sin(\theta_1 + \theta_2 + \theta_3)$. The symbol $\mathbf{C}(\boldsymbol{\theta})$ represents the Coriolis and centrifugal forces within the system. g stands for the acceleration due to gravity.

For the total torque $\boldsymbol{\tau}(t)$, it consists of three components for each joint. The first component is the passive torque $\boldsymbol{\tau}_{\text{passive}}(t)$, which represents the contributions of intrinsic tonic joint stiffness and damping. The second component is the active torque $\boldsymbol{\tau}_{\text{active}}(t)$, which is designed to counteract the torque induced by external disturbances at each joint. The third component is the noise torque $\boldsymbol{\tau}_{\text{noise}}(t)$, which is used to simulate external disturbances of each joint. $\boldsymbol{\tau}(t)$ can be described as follows:

$$\boldsymbol{\tau}(t) = \boldsymbol{\tau}_{\text{passive}}(t) + \boldsymbol{\tau}_{\text{active}}(t) + \boldsymbol{\tau}_{\text{noise}}(t) \quad (20)$$

where $\boldsymbol{\tau}(t) = [\tau_1, \tau_2, \tau_3]^{\text{T}}$, $\boldsymbol{\tau}_{\text{passive}} = [\tau_{\text{p1}}, \tau_{\text{p2}}, \tau_{\text{p3}}]^{\text{T}}$, $\boldsymbol{\tau}_{\text{active}} = [\tau_{\text{a1}}, \tau_{\text{a2}}, \tau_{\text{a3}}]^{\text{T}}$ and $\boldsymbol{\tau}_{\text{noise}}(t) = [\tau_{\text{n1}}, \tau_{\text{n2}}, \tau_{\text{n3}}]^{\text{T}}$. Each noise torque component $\tau_{\text{n}i}$ is calculated as follows:

$$\tau_{\text{n}i} = \left(\frac{\sigma}{60}\right)\xi\sqrt{\frac{1}{T}} \quad (21)$$

where σ denotes a variable parameter, ξ is a uniformly distributed random number between 0 and 1, and T represents the sampling time.

The parameters of this TIP model were derived from a range of anthropometric measurements documented in previous papers [47], [48]. This ensures that the selected parameters are both appropriate and accurate for our simulations. The detailed parameters are listed in Fig. 1.

2) VSIP Model: The VSIP model constitutes another core component of the HTIP model. Unlike the TIP model, which encapsulates all the crucial joints and links for simulating human quiet stance, the VSIP aims to simplify and simulate the overall dynamics of the human body in the sagittal plane maintaining balance by focusing on the dynamic changes of the entire body's CoM. This approach is designed to mimic more natural dynamics of human balance maintenance. The VSIP model and its specific parameters used for simulations are detailed in Fig. 2.

The detailed dynamic equation of the VSIP model is described as follows:

$$I\ddot{\theta}_{\text{CoM}}(t) = mgh\theta_{\text{CoM}}(t) + \tau_{\text{passive}}(t) + \tau_{\text{active}}(t) + \tau_{\text{noise}}(t) \quad (22)$$

where I is the moment of inertia of the human body around the ankle. The tilt angle of the human body in the sagittal plane during quiet stance, denoted as $\theta_{\text{CoM}}(t)$, varies over time. The approximation $\sin(\theta_{\text{CoM}}(t)) \approx \theta_{\text{CoM}}(t)$ is made, suitable for low angles. Additionally, this angle's first and second order derivatives correspond to angular velocity $\dot{\theta}_{\text{CoM}}(t)$ and angular acceleration $\ddot{\theta}_{\text{CoM}}(t)$ respectively. m, g, and h are the mass of the human body, the gravity acceleration, and the distance from the ankle joint to the CoM of the human body, respectively.

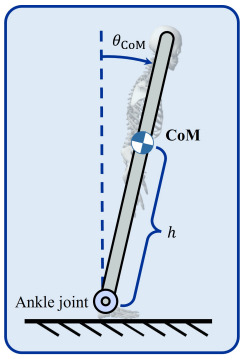

Symbol	Description	Value
m	Mass of total body	73.1851 kg
h	Total CoM's distance from the ankle axis	1.0194 m

Fig. 2. VSIP model framework in the sagittal plane and simulation parameters.

3) HTIP Model: The core advantage of the HTIP model lies in its comprehensive integration of three crucial joints: the ankle, knee, and hip. This integration allows for a thorough representation of the interactions between the entire body and external forces such as gravity and disturbances. However, directly calculating the feedback torque based on the motion state of each corresponding body part associated with these joints involves complex computations, which do not align with the way the human brain processes information. Therefore, to simplify the problem, we utilize the VSIP model to determine the motion state of the body's CoM and then calculate the required feedback torque based on this state. The calculated torque is subsequently fed back into the TIP model to simulate the body's dynamic response after receiving the feedback. The framework of the designed HTIP model is shown in Fig. 3.

B. Neural Control Model

The neural control model is another crucial component of the neuromechanical model for human quiet stance. Based on the posture and dynamic information of the human body, this model simulates neural feedback mechanisms that adjust the torque output of muscles, in response to external disturbances and to maintain postural stability. Although various neural control models integrated with human body models have been proposed, they often fail to accurately reflect the natural postural sway of the human body's CoM. Typically, the simulated CoM trajectory remains near the origin, which does not align with the natural phenomenon of human standing and usually requires higher energy consumption to maintain the posture. Consequently, this paper adopts an intermittent control model based on the motion state of the human body's CoM, aiming to reduce energy consumption and more accurately simulate

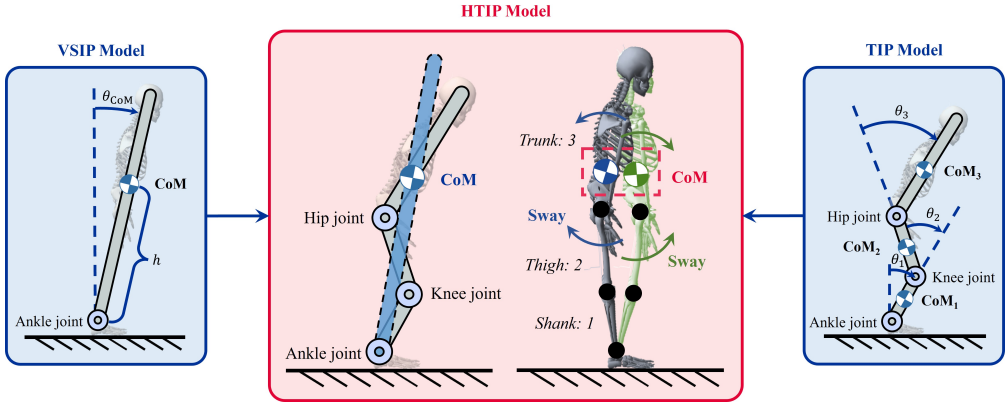

Fig. 3. The illustration of three models used to simulate and analyze the dynamics of human quiet stance. The VSIP model, depicted on the left, serves as a computational simplification tool, representing the overall dynamics of the body's CoM. Unlike traditional SIP models, where the CoM corresponds directly to a single segment, this virtual model's CoM actually represents the comprehensive CoM of the entire TIP model, mirroring the overall gravitational center of the human body. The TIP model, shown on the right, provides a detailed simulation of the dynamics of the ankle, knee, and hip joints in the sagittal plane, along with the corresponding lower leg (shank), upper leg (thigh), and upper body (trunk) segments, during quiet stance. This model captures the interplay between these joints and segments, offering a more thorough representation of how the entire body interacts with gravitational forces and external disturbances. The HTIP model, depicted in the center, integrates both the VSIP and TIP models to offer a balanced framework for simulating human standing dynamics, combining the simplicity of the single pendulum for CoM representation with the detailed mechanics of the triple pendulum, resulting in a comprehensive model that reflects the nuanced interactions between different body segments.

natural human quiet stance. This control model consists of two main parts: stiffness and damping control, and state-dependant activation criteria.

1) Stiffness and Damping Control: In the field of neuromechanical modeling for human quiet stance in the sagittal plane, stiffness and damping control are widely implemented within human body models. Stiffness control is achieved through the proportional (P) component, which generates a feedback force proportional to the deviation from the body's ideal posture. This mechanism simulates the biomechanical response of the human body, wherein joints naturally increase their stiffness to resist disturbances perceived as deviations from a balanced state. Damping control is implemented through the derivative (D) component, which focuses on the rate of posture change and adds system damping to suppress excessive motion or oscillations. The equation for stiffness and damping control, which provides feedback torque, can be described as follows:

$$\tau_{\text{active}}(t) = -P(t)\theta_{\text{CoM}\Delta}(t) - D(t)\dot{\theta}_{\text{CoM}\Delta}(t) \tag{23}$$

where $\tau_{\text{active}}(t)$ is the active feedback torque through the CNS with time delay Δ. $P(t)$ and $D(t)$ represent the proportional and derivative feedback gains, respectively. $\theta_{\text{CoM}\Delta}(t)$ and $\dot{\theta}_{\text{CoM}\Delta}(t)$ are the delayed tilt angle and angular velocity of the human body due to the neural transmission delay, where $\theta_{\text{CoM}\Delta}(t) = \theta_{\text{CoM}}(t-\Delta)$ and $\dot{\theta}_{\text{CoM}\Delta}(t) = \dot{\theta}_{\text{CoM}}(t-\Delta)$.

In addition, the elastic properties of the ankle, knee and hip muscles provide the body with a passive torque to maintain standing balance, which can be described as follows:

$$\boldsymbol{\tau}_{\text{passive}}(t) = -\mathbf{K}\boldsymbol{\theta}(t) - \mathbf{B}\dot{\boldsymbol{\theta}}(t) \tag{24}$$

where $\mathbf{K} = \text{diag}[K_a, K_k, K_h]$ is passive elastic coefficient matrix of ankle, knee and hip joints, $\mathbf{B} = \text{diag}[B_a, B_k, B_h]$ is passive viscosity coefficient matrix of ankle, knee and hip joints.

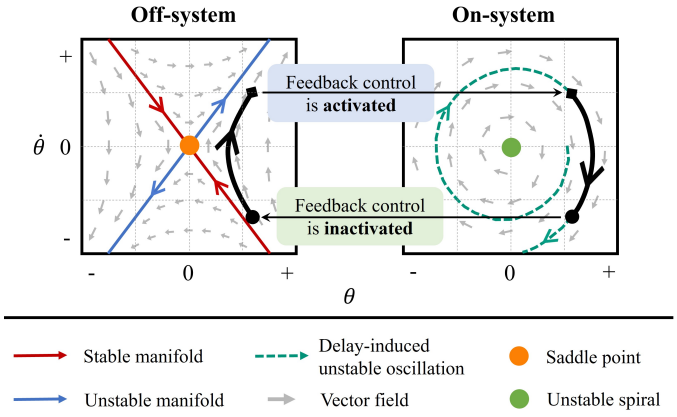

Fig. 4. The illustration of the impact of intermittent control on a SIP model of human quiet stance in the sagittal plane, comparing it through two state phase portraits. A state phase portrait is a dynamical tool that represents the trajectories of a system's states (angle $\boldsymbol{\theta}$ and angular velocity $\dot{\boldsymbol{\theta}}$) over time, revealing the system's stability and dynamic behavior. In the left subfigure, the controller is in the 'Off' state. The diagram marks two main manifolds: a stable manifold, represented by a red line, near to which the pendulum's momentum drives the state towards the equilibrium point, the origin. In contrast, when near to the unstable manifold (represented by a blue line) the state diverges away from the origin. This origin is also referred to as a saddle point. The right subfigure shows the controller in the 'On' state. Due to delays in neural signal transmission and physiological response times that prevent the controller from responding immediately and providing appropriate torque, if the active control is maintained continuously, the oscillatory movement gradually increase in amplitude and becomes an unstable spiral. Therefore, based on how close the human body's CoM movement state $(\boldsymbol{\theta}, \dot{\boldsymbol{\theta}})$ is to the stable and unstable manifolds, it is necessary to determine the controller's state to stabilize human standing by alternating between stable and unstable states.

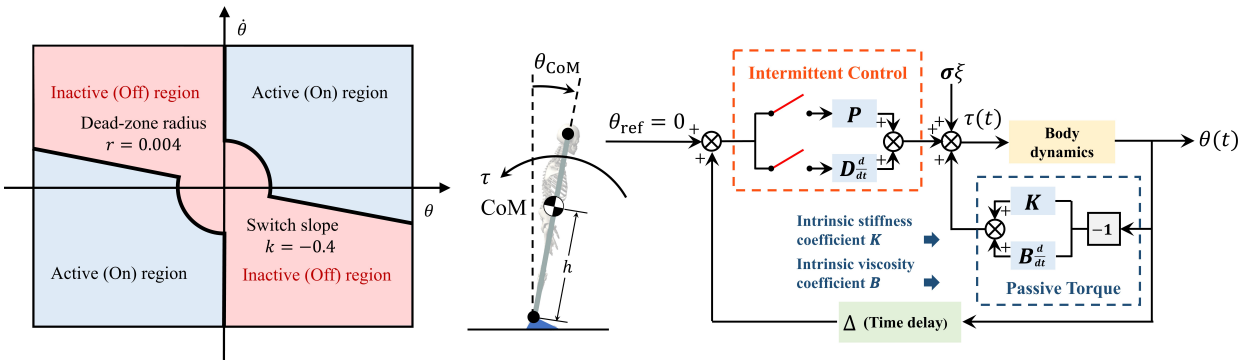

Fig. 5. The illustration of the intermittent neural feedback control mechanism for stabilizing human quiet stance in the sagittal plane, comparing two subfigures. The left subfigure depicts the conditions for activating the neural feedback controller, based entirely on the state of the human body's CoM $(\boldsymbol{\theta}, \dot{\boldsymbol{\theta}})$. The control regions are delineated by stable/unstable manifolds with a set slope of -0.4. The pink area represents the inactive (off) state, where the controller does not activate when the CoM is within this region. Conversely, the blue area indicates the active (on) state, where the controller is activated. The central circular inactive area reflects the brain's perceptual dead zone when the CoM approaches the origin—despite nearing the center point, the controller should not activate, mimicking the natural perceptual limitations of human positional accuracy. The right subfigure shows a block diagram of intermittent control for human standing. The stability of the human body relies not only on active torque generated by intermittent control but also on passive torque and the intrinsic stiffness and viscosity coefficients of joints and muscles. Feedback signals from the body's CoM are sent back to the brain for a new round of decision-making on whether to activate the controller. However, due to delays in neural signaling and physiological responses, these feedback signals are delayed, affecting the immediacy of control decisions.

2) State-Dependant Activation Criteria: In the neuromechanical modeling of human quiet stance in the sagittal plane, unlike the continuous activation seen in stiffness and damping control, the neural control mechanism typically adopts an intermittent activation form. Fig. 4 shows the impact of intermittent control on the mechanism of human quiet stance through state phase portraits. The specific intermittent neural feedback control mechanism for stabilizing human quiet stance is shown in Fig. 5. If $\theta_{\text{CoM}\Delta}\left(\dot{\theta}_{\text{CoM}\Delta} - k\theta_{\text{CoM}\Delta}\right) > 0$ and $\theta^2_{\text{CoM}\Delta} + \dot{\theta}^2_{\text{CoM}\Delta} > r^2$, then $\tau_{\text{active}}(t)$ is as shown in Equation (23), otherwise $\tau_{\text{active}}(t) = 0$, where $k = -0.4$ is the switching slope and $r = 0.004$ is the radius of the circular dead-zone. This control strategy effectively maintains dynamic equilibrium, alleviates muscle fatigue, responds to sensory feedback, and enhances energy efficiency by momentarily adjusting muscle activity. Specifically, even when attempting to remain still, the human body needs to make minor muscle adjustments to counteract gravity and external disturbances; by intermittently activating different muscle groups, the body efficiently distributes the continuous strain, preventing overuse injuries. Moreover, muscle activity is often a direct response to feedback from sensory systems such as the visual, vestibular (inner ear balance system), and proprioceptive (sense of body position) systems. Intermittent activation helps the body conserve energy while maintaining postural stability. Experimental studies showed that the switching on and off of neural feedback control is closely related to the state of the human body's CoM [33], [41]. Therefore, we developed an intermittent controller based on the state of the center of mass motion, which regulates the HTIP model to simulate postural sway during human quiet stance. The parameters of HTIP model used for subsequent simulation is shown in Table I.

C. Kinematic Data Acquisition

Experimental data were acquired with the aim of validating the developed model.

TABLE I
PARAMETERS OF HTIP MODEL USED FOR HUMAN QUIET STANCE SIMULATION.

Symbol	Description	Value
K_a	Passive elastic coefficient at ankle	$0.8mgh$
B_a	Passive viscosity coefficient at ankle	50
K_k	Passive elastic coefficient at knee	$0.9mgh$
B_k	Passive viscosity coefficient at knee	50
K_h	Passive elastic coefficient at hip	$0.9mgh$
B_h	Passive viscosity coefficient at hip	50
P	Proportional parameter of the intermittent controller	$0.95mgh$
D	Derivative parameter of the intermittent controller	250
T	Sampling time	0.001 s
σ	Noise variable parameter	30

TABLE II
PARTICIPANT DETAILS

Subject	Gender	Age (years)	Height (cm)	Weight (kg)
1	Male	25	169	63
2	Male	26	174	82
3	Male	24	180	66
4	Male	25	173	61
5	Male	24	171	65
6	Male	23	174	64
7	Female	23	164	49
8	Female	24	170	51

1) Subjects: The study recruited 8 young participants, comprising 6 males and 2 females. Table II provides detailed information on the age, height, and weight of each participant. These individuals reported no history of health conditions affecting locomotion, neurological functions, or any other health issues that could potentially influence their performance. Prior to participation, all participants provided informed consent. The study received approval from the Imperial College London Research Ethics Committee (Reference: 19IC5641).

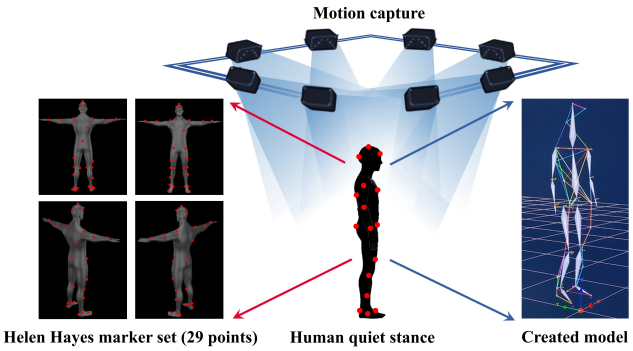

Fig. 6. The illustration of the experimental setup for capturing the dynamics of human standing in the sagittal plane using the Nokov 3D Optical Camera System and the Helen Hayes full-body with head marker set [49]. On the left side of the image, the Helen Hayes marker set is displayed, consisting of 29 points used to precisely track the motion of human joints and key body parts. Throughout the standing process, eight Nokov 3D Optical Cameras positioned above the subject's head record the posture in real-time. During this process, subjects were instructed to stand naturally, avoiding excessive focus or tension. Subjects' arms were to hang naturally by their sides, eyes open, with gaze directed straight ahead. On the right side of the image, the real-time human posture reconstruction is rendered using Nokov's Xingying 3.2 software.

2) Experimental Setup: To accurately capture the dynamics of postural adjustments during quiet stance in the sagittal plane, this study utilized the Nokov 3D Optical Motion Capture System, as shown in Fig. 6. This system is capable of precisely tracking the human body in three-dimensional space and measuring corresponding motion parameters. The Helen Hayes full-body with head marker set was adopted, which can be used to calculate the CoM of the human body, and calibration of the capture volume was conducted before each session. During the experiments, subjects were instructed to stand quietly on a flat surface, with their arms naturally hanging by their sides and eyes looking straight ahead.

3) Experimental Protocol: The experimental protocol and setup are shown in Fig. 7, which contains five steps: Pre-experiment, Preparation, Action, Repetition and Post-experiment. Before the experiment commenced, subjects were asked to sit on a chair without backrest and armrest support, placing their hands on their thighs for 30 seconds to facilitate physiological and psychological stabilization. After this preparation phase, subjects were required to stand up from the chair without using the chair's arms and then to maintain a quiet stance posture for 120 seconds. During this process, it was emphasized that subjects should stand naturally, avoiding excessive focus or tension to simulate everyday standing scenarios as closely as possible. Subjects' arms were to hang naturally by their sides, with eyes open and gaze directed straight ahead. To ensure data reliability and account for individual variability, each participant was required to complete 5 repetitions of the procedure. The more stable 60 seconds from the 120-second standing period were selected for validating and comparing the model, as the initial phase of the 120 seconds may involve physiological adjustments. This ensures that steadier data are used for more reliable analysis.

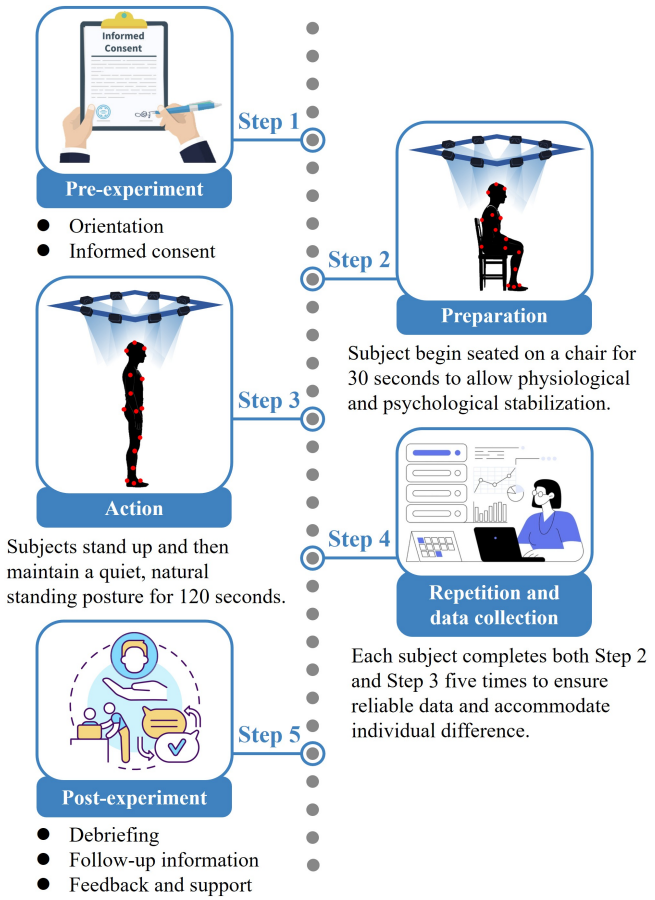

Fig. 7. Experimental Protocol. The protocol includes five steps: (1) Pre-experiment: orientation and informed consent; (2) Preparation: 30 seconds of seated stabilization; (3) Action: 120 seconds of quiet standing posture; (4) Repetition: Steps 2 and 3 repeated five times for data collection; (5) Post-experiment: debriefing, follow-up information, feedback and support.

III. Results

In order to validate our HTIP model, two types of simulations were conducted with different initial conditions. Simulation 1 represented the HTIP model starting from $\theta_{\mathrm{CoM}} = 0$, simulating human natural postural sway near the equilibrium point. Simulation 2 started from $\theta_{\mathrm{CoM}} = 0.005$, simulating whether the model can maintain a normal and stable natural postural sway when starting slightly away from the equilibrium. In both cases, the initial $\dot{\theta}_{\mathrm{CoM}}$ was set to 0 to ensure consistency. The results of these simulations are compared with experimental data collected from eight subjects. The following sections provide a detailed analysis of the time-series data, power spectral density (PSD), and phase portraits to assess the HTIP model's performance in replicating human postural sway dynamics. These metrics were selected because they are commonly used to understand and analyze human standing behavior [18], [50], [51] and they are also extensively applied in quantifying the neuromechanical model of human quiet stance performance [25], [38], [46], [52].

Fig. 8 and 9 present the time-series data of θ_{CoM} and $\dot{\theta}_{\mathrm{CoM}}$ for the eight subjects alongside the two simulation outputs. Fig. 8A shows that the time-series of θ_{CoM} for the subjects

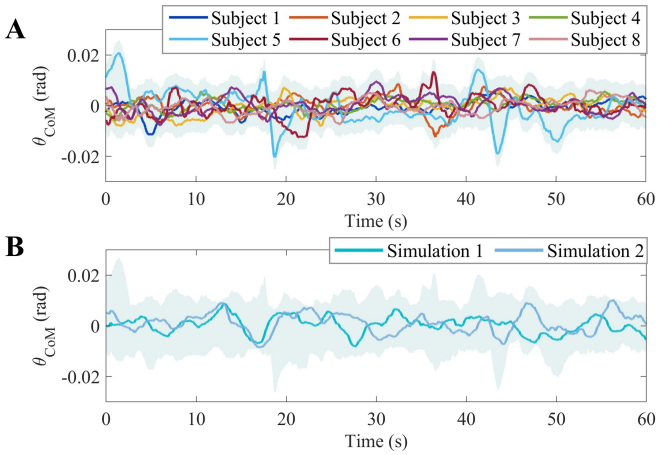

Fig. 8. **A.** The variation in $\boldsymbol{\theta}_{\text{CoM}}$ for 8 subjects during static standing was recorded using a motion capture system. Each curve represents the time-series data of $\boldsymbol{\theta}_{\text{CoM}}$ for an individual subject. The shaded region includes all the curves, indicating the range of variations across all participants. **B.** The 2 types of simulated dynamics of $\boldsymbol{\theta}_{\text{CoM}}$ over time for the HTIP model under state-dependent intermittent control. Each line represents the trajectory of $\boldsymbol{\theta}_{\text{CoM}}$ as calculated by the model, demonstrating how the simulated dynamics align with the real human data, which is represented by the shaded region.

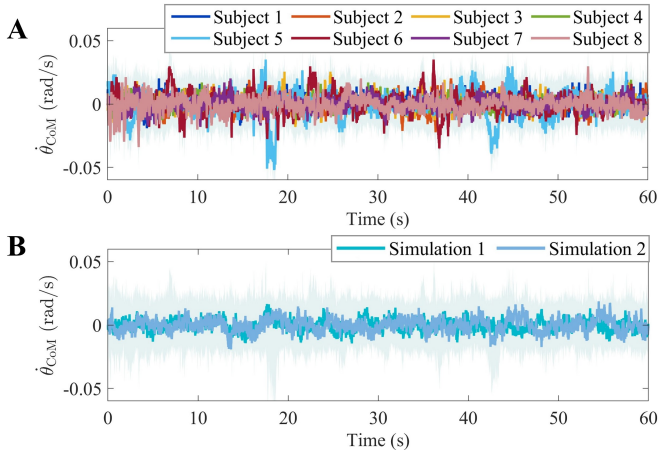

Fig. 9. **A.** $\dot{\boldsymbol{\theta}}_{\text{CoM}}$ for 8 subjects during static standing was recorded using a motion capture system. Each line in the graph represents the time-series data of $\dot{\boldsymbol{\theta}}_{\text{CoM}}$ for an individual subject throughout the experiment. The shaded region includes all the curves, indicating the overall range of $\dot{\boldsymbol{\theta}}_{\text{CoM}}$ variations among all participants. **B.** The 2 kinds of simulated $\dot{\boldsymbol{\theta}}_{\text{CoM}}$ over time for the HTIP model under state-dependent intermittent control. Each line represents the time-series of $\dot{\boldsymbol{\theta}}_{\text{CoM}}$ as generated by the model, placed within the shaded region that represents the angular velocity data from eight subjects during static standing.

exhibit low-frequency oscillations with amplitude variations between individuals. These oscillations are tightly bounded, staying mostly within a range of ±0.02 rad. Similarly, the simulated data in Fig. 8B shows comparable oscillations with similar amplitude ranges. Notably, both Simulation 1 and Simulation 2 closely replicate the fluctuations observed in the experimental data, indicating that the HTIP model can effectively simulate natural postural sway.

For the $\dot{\theta}_{\text{CoM}}$ shown in Fig. 9A and Fig. 9B, the experimental data shows faster corrections during postural adjustments, with $\dot{\theta}_{\text{CoM}}$ oscillating between ±0.04 rad/s. Both simulations display comparable velocity ranges, again aligning closely with the experimental findings. This suggests that the model captures the velocity dynamics of postural adjustments, an important aspect of balance control.

Fig. 10 and 11 present the PSD analysis for θ_{CoM} and $\dot{\theta}_{\text{CoM}}$. PSD analysis is crucial for understanding the dynamics of postural control as it evaluates how the power of a signal is distributed across different frequencies. In the context of quiet standing, PSD helps to characterize the body's response to balance perturbations, with lower frequencies indicating slow and continuous adjustments to maintain balance, and higher frequencies representing faster, more corrective actions. In both figures, linear regression is applied to the log-log plots of the PSD to estimate the slope (β). The slope provides a quantitative measure of how power is distributed across different frequencies, allowing for a direct comparison between experimental data and simulation results.

In the experimental data from Fig. 10A, the PSD slopes for θ_{CoM} range from -3.41 to -2.60, indicating that low-frequency components dominate postural control. In the simulations from Fig. 10B, the PSD slopes are -3.224 and -3.216 for Simulation 1 and 2, respectively. These slopes are within the range observed in the experimental data, demonstrating that the HTIP model replicates the distribution of energy across frequencies and the dominance of low-frequency adjustments in human balance.

For $\dot{\theta}_{\text{CoM}}$ from Fig. 11, the PSD slopes in the experimental data range from -1.61 to -0.84, showing a greater presence of higher frequency components, which correspond to faster corrective actions. The simulations produced slopes of -1.342 and -1.321, aligning with the experimental data. This close match in both frequency domains supports the model's accuracy in replicating not only slow adjustments but also rapid dynamic responses in postural control.

The direct comparison of these slope values is effectively visualized in Fig. 12, which uses bar graphs to compare the PSD slopes of θ_{CoM} and $\dot{\theta}_{\text{CoM}}$ between the subjects and simulations. The bar plots provide a clear visualization of how closely the simulated slopes align with those of the subjects.

Fig.13A presents the phase portraits of θ_{CoM} versus $\dot{\theta}_{\text{CoM}}$ for eight subjects during quiet standing. Each subject exhibits a stable and similarly bounded trajectory, forming saddle-shaped loops in the phase space. These variations in loop size and shape across individuals reflect the natural differences in balance control strategies, but overall, the trajectories remain within a controlled range, indicating effective postural stability.

Fig. 13B shows the phase portraits for the two simulations. Both Simulation 1 and Simulation 2 exhibit stable, bounded oscillations. Importantly, the boundaries of these trajectories closely resemble those of Subject 7. The size and shape of the saddle-shaped loops in both simulations are highly similar to those of Subject 7, indicating that the HTIP model can replicate not only the overall shape of the oscillations but also the boundary conditions that define stable postural control.

Fig. 14 presents box plots comparing the average values and variances of θ_{CoM}, $\dot{\theta}_{\text{CoM}}$, joint angles ($\theta_1$, θ_2, θ_3) and angular velocities ($\dot{\theta}_1$, $\dot{\theta}_2$, $\dot{\theta}_3$) between the experimental subjects and

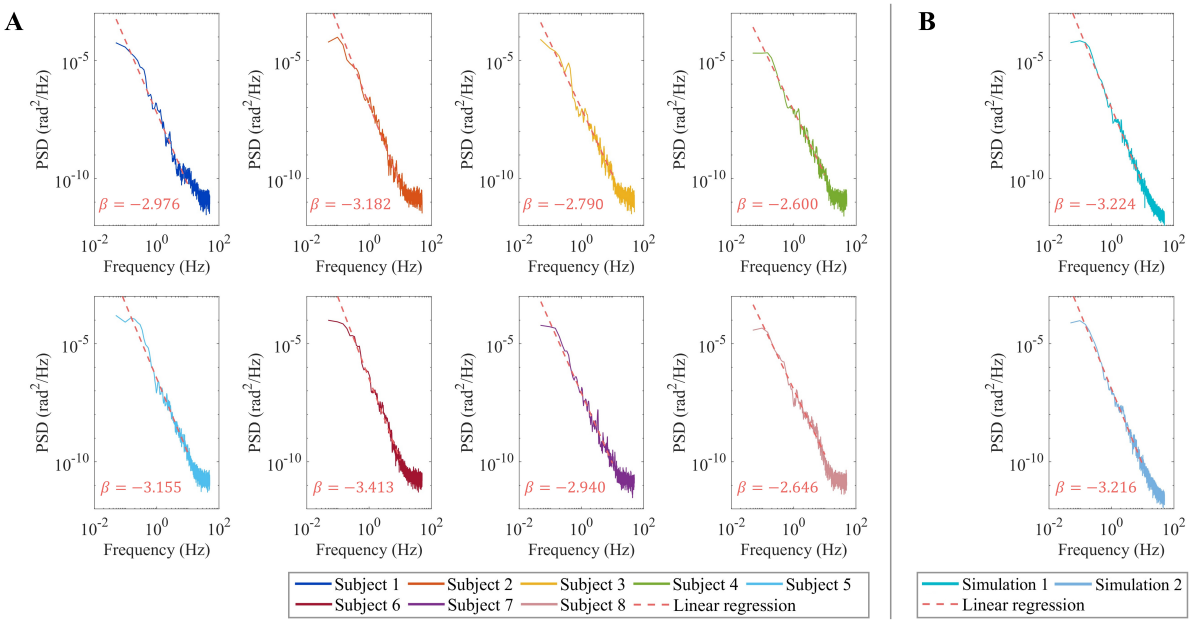

Fig. 10. **A.** PSD of θ_{CoM} for eight subjects during quiet standing. Each subplot corresponds to an individual subject, with the blue solid lines showing the PSD and the red dashed lines representing the linear regression fit. The slope (β) for each subject is indicated on the plot. **B.** PSD for two simulated data sets, showing the results of the HTIP model simulations.

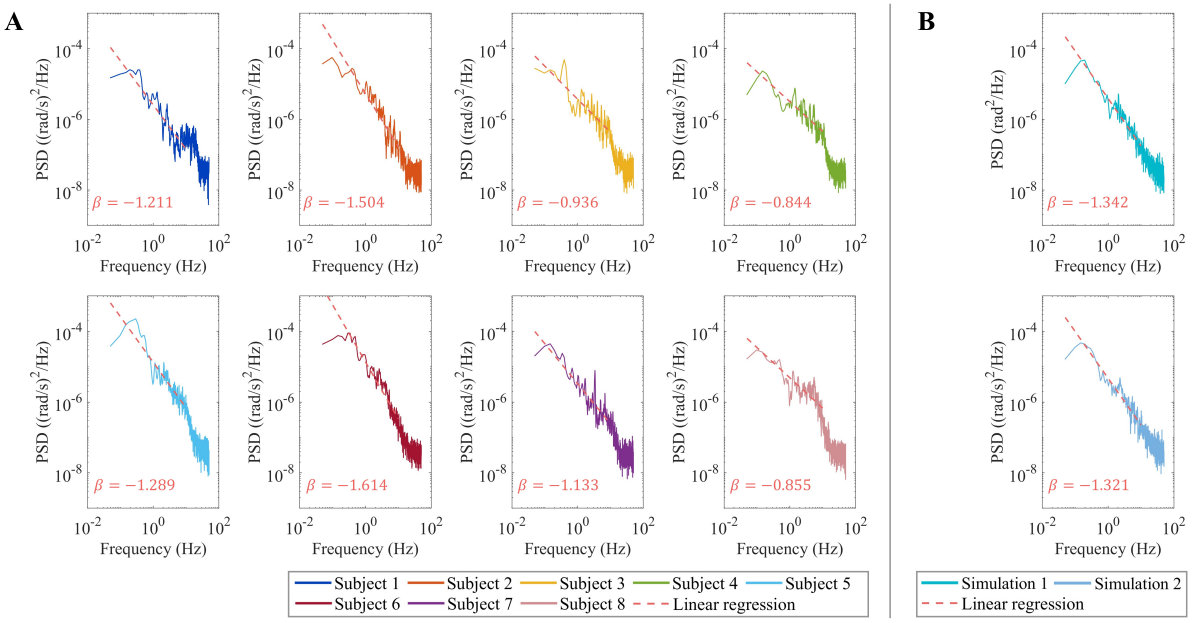

Fig. 11. **A.** PSD of $\dot{\theta}_{\text{CoM}}$ for eight subjects during quiet standing. Each subplot corresponds to an individual subject, with the blue solid lines showing the PSD and the red dashed lines representing the linear regression fit. The slope (β) for each subject is indicated on the plot. **B.** PSD for two simulated data sets, showing the results of the HTIP model simulations.

the simulations during quiet standing. The average angle values for both subjects and simulations are centered near zero, indicating that, on average, both the subjects and the HTIP model maintain an upright posture with minimal deviation from equilibrium. This closeness to zero demonstrates the effectiveness of the HTIP model in replicating natural equilibrium postures during quiet standing.

In terms of variance, both the experimental and simulation results reveal that the hip joint (θ_3) shows the largest variance, indicating its critical role in dynamic postural adjustments. The model closely matches the observed variance at the hip, reflecting its ability to replicate the hip's contribution to maintaining balance through larger, more variable movements. Additionally, the ankle (θ_1) and knee (θ_2) joints show lower variances in both the experimental and simulation data, reflecting the more stable control of these joints during quiet standing. Similarly, for angular velocities, the simulations and experimental results show a comparable trend: the hip joint ($\dot{\theta}_3$) exhibits the highest variability, while $\dot{\theta}_{\text{CoM}}$ and ankle joints display more stable velocity control. The HTIP model accurately captures these

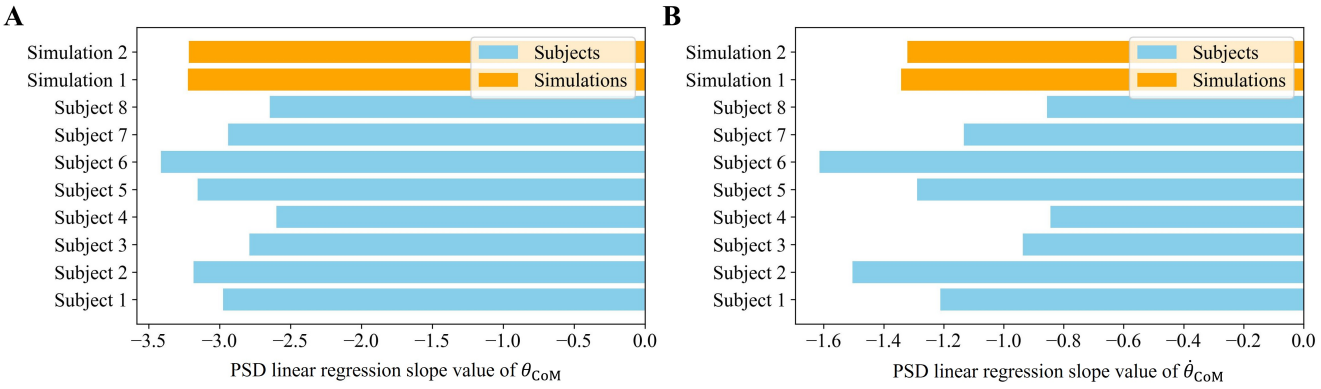

Fig. 12. **A.** Comparison of the PSD linear regression slope values of θ_{CoM} for subjects and simulations, showing the simulations are very similar to the subject data in terms of PSD slope. **B.** Comparison of the PSD linear regression slope values of $\dot{\theta}_{CoM}$ for subjects and simulations, showing the simulations are very similar to the subject data in terms of PSD slope.

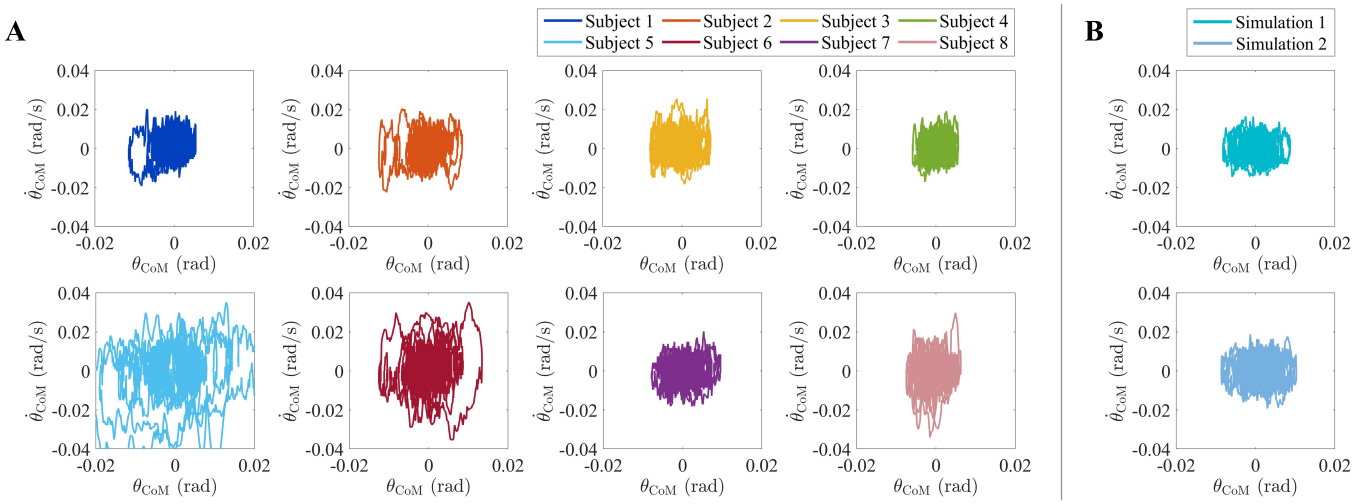

Fig. 13. **A.** The state phase portraits of θ_{CoM} and $\dot{\theta}_{CoM}$ for eight subjects during static standing, obtained via motion capture technology, are presented. Each plot represents the dynamic trajectory of one subject, depicting the temporal evolution of θ_{CoM} and $\dot{\theta}_{CoM}$ within a two-dimensional phase space. This collection of portraits offers a detailed analysis of individual variability and common patterns in postural stability and control among the subjects. **B.** State phase portraits for two simulations, which can be directly compared to the subjects' data, proving the model's ability to replicate key features of human postural control.

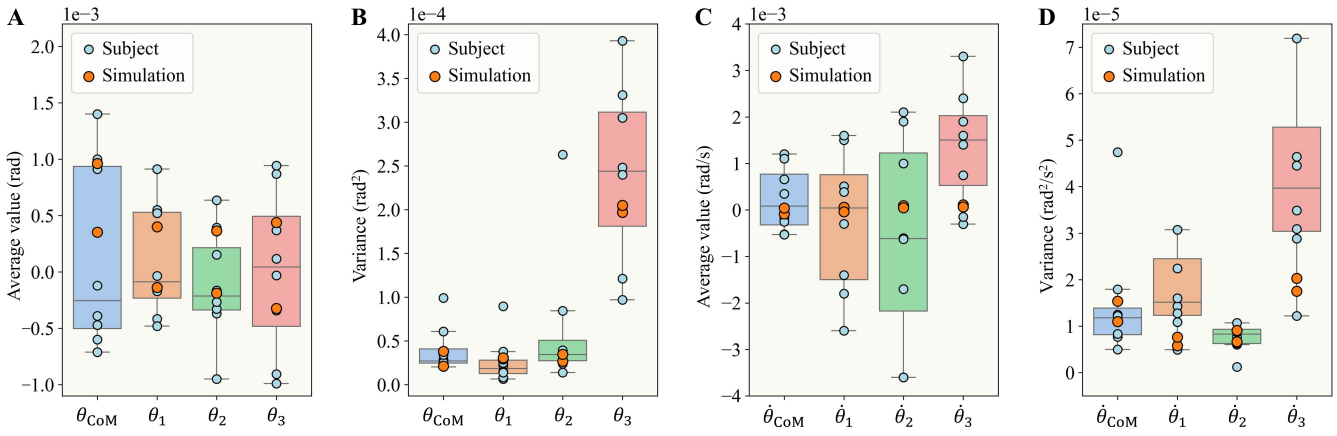

Fig. 14. Box plots comparing average values and variances of angles and angular velocities between subjects and simulations during static standing. **A.** Average angle values, **B.** angle variances, **C.** average angular velocities, and **D.** variances of angular velocities for the CoM, ankle, knee, and hip joints. The alignment between simulation (orange circle) and experimental results from subjects (blue circle) demonstrates the validity of the proposed HTIP model.

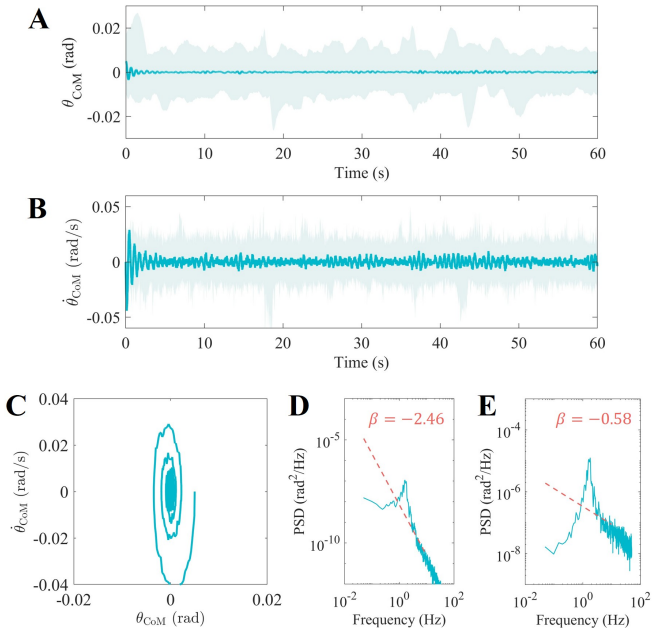

Fig. 15. Results from continuous control theory applied to the TIP model. **A.** Time-series plot of θ_{CoM}. **B.** Time-series plot of $\dot{\theta}_{\text{CoM}}$. **C.** State phase portrait of θ_{CoM} versus $\dot{\theta}_{\text{CoM}}$. **D.** PSD of θ_{CoM}, with a slope of -2.46. **E.** PSD of $\dot{\theta}_{\text{CoM}}$, with a slope of -0.58.

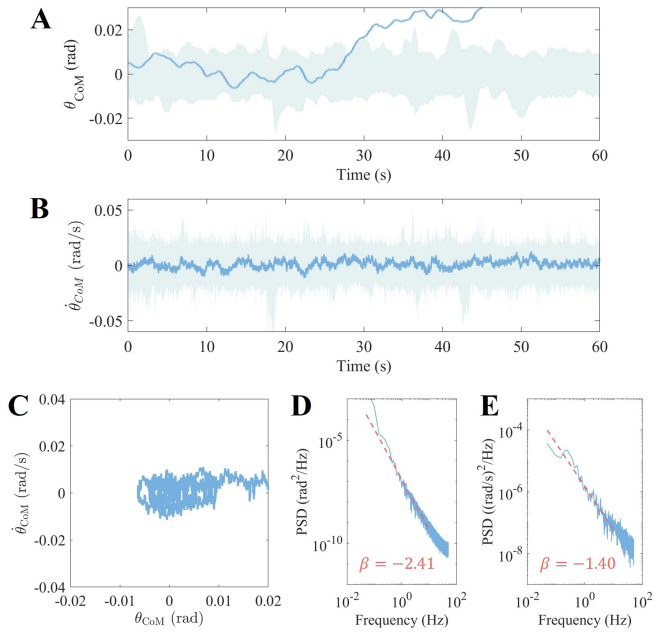

Fig. 16. Results from traditional intermittent control theory applied to the TIP model. **A.** Time-series plot of θ_{CoM}. **B.** Time-series plot of $\dot{\theta}_{\text{CoM}}$. **C.** State phase portrait of θ_{CoM} versus $\dot{\theta}_{\text{CoM}}$. **D.** PSD of θ_{CoM}, with a slope of -2.41. **E.** PSD of $\dot{\theta}_{\text{CoM}}$, with a slope of -1.40.

variances, aligning with the experimental data, particularly for the hip, showing its ability to simulate both slow adjustments and rapid corrective actions.

In addition to evaluating the HTIP model's performance, we conducted two comparative experiments to further highlight the advantages of the proposed model. The first experiment applied continuous control theory to stabilize the TIP model, while the second experiment utilized traditional intermittent control theory.

In the continuous control experiment, the model maintained a stable postural sway, as demonstrated by the time-series plots of θ_{CoM} and $\dot{\theta}_{\text{CoM}}$ from Fig. 15A and Fig. 15B. The state phase portrait in Fig. 15C shows that the system started from $\theta_{\text{CoM}} = 0.005$ and converged to the origin, forming small, elliptical oscillations. This convergence to zero indicates effective stabilization of the system under continuous control. However, the PSD curves in Fig. 15D and Fig. 15E, with slopes of -2.46 for θ_{CoM} and -0.58 for $\dot{\theta}_{\text{CoM}}$, differ from the experimental PSD curves observed in human subjects [53], [54], indicating that the frequency components are not consistent with natural postural sway.

In contrast, the traditional intermittent control experiment failed to maintain stability over time. The time-series plots of θ_{CoM} and $\dot{\theta}_{\text{CoM}}$ from Fig. 16A and Fig. 16B. show increasing oscillations, indicating that the system drifted away from equilibrium. The state phase portrait in Fig. 16C exhibits unbounded, irregular trajectories, further confirming the loss of control. As shown in Fig. 16D, the curve and slope of PSD are both inconsistent with the natural postural sway observed in human subjects. [38], [55]

IV. Discussion

This study integrates the HTIP model with a state-dependent intermittent neural control strategy, employing neuromechanical modeling techniques to successfully simulate the natural postural sway observed during quiet stance in humans. The consistency of the model with actual human standing posture was validated across three dimensions: time domain, frequency domain, and state phase portrait. To visually demonstrate this consistency, the paper employs bar graphs and box plots to compare the model predictions of postural sway with actual observational data. These results explicitly demonstrate the model's capability to replicate the natural sway observed in human quiet stance.

In the time-domain analysis of Fig. 8 and 9, it is observed that during human quiet stance, both θ_{CoM} and $\dot{\theta}_{\text{CoM}}$ oscillate within a relatively small, limited range. This indicates that muscles are not constantly in a highly activated state while standing but instead allow for minimal, controlled postural sway within a defined range. The CNS activates muscles to return the body to its original position only in cases of excessive forward or backward tilting, which is a key characteristic of the natural postural sway in quiet human stance. Conversely, if the muscles were to remain highly activated, keeping the body rigid, the θ_{CoM} would not exhibit any oscillations, contradicting the natural behavior of standing in humans. This intermittent muscle activation pattern has been observed through both surface and intramuscular electromyography, with particular prominence in the gastrocnemius and soleus muscles [22], [56].

The θ_{CoM} and $\dot{\theta}_{\text{CoM}}$ signals in human quiet standing posture were additionally transformed into their frequency-domain representations using PSD analysis, as illustrated in Fig. 10

and 11. Linear regression analysis revealed that the slopes of the angle signals ranged from -3.41 to -2.60, and those of the angular velocity signals from -1.61 to -0.84. The steeper negative slopes of the angle signals indicate a significant decrease in PSD values at higher frequencies, demonstrating the system's strong suppression of high-frequency disturbances, namely, the energy of high-frequency components is relatively low. This suggests that although all frequency components contribute to the total signal energy, the low-frequency components have a relatively greater impact.

Moreover, these findings suggest that neural control predominantly operates via low-frequency actions. The nervous system activates muscles or adjusts neural signals when necessary and allows them to rest when not required, thereby optimizing energy utilization. This control strategy reduces the energy consumption needed to maintain continuous muscle tension, thereby helping to prevent muscle fatigue and enhance overall efficiency.

Notably, it also shows that the system's response may depend on its current state. For instance, when the system is near the stable equilibrium point, the controller may decrease activation frequency or intensity. Conversely, when the system deviates from the equilibrium point, the controller may increase activation frequency or intensity. This state-dependent regulation could explain the observed characteristic variations in the slopes of the PSD linear regression.

Furthermore, the state phase portraits from Fig. 13 reveal that the HTIP model effectively simulates human postural control during quiet standing. The saddle-shaped trajectories represent the dynamic balance between the CoM displacement and velocity, showing how both the experimental subjects and the model maintain stability through controlled, bounded oscillations. Near the equilibrium, oscillations are smaller and more controlled; however, greater deviations lead to more pronounced corrective actions, reflecting the body's natural response to balance disturbances. This behavior aligns with human postural control, where muscles intermittently activate to correct larger deviations, while remaining relaxed during small fluctuations. The model accurately captures this state-dependent control mechanism, demonstrating its effectiveness in replicating the natural balance dynamics observed in human subjects.

Therefore, the HTIP model and the state-dependent intermittent neural control strategy proposed in this study successfully reproduce key characteristics of human quiet standing, including time-domain responses, frequency-domain features, and phase trajectories. This model addresses the challenges faced by existing intermittent control models in stabilizing the triple inverted pendulum that represents the human body system. As shown in Fig. 15, traditional neural control models employ continuous controllers to maintain the stability of the triple inverted pendulum, which contradicts the intermittent nature of muscle activity during human quiet standing. Conversely, directly applying traditional intermittent control strategies fails to stabilize the triple inverted pendulum, as illustrated in Fig. 16, rendering it incapable of maintaining human stance, namely, stability cannot be achieved using only traditional intermittent controllers [41], [54].

The primary reason for this failure is that traditional intermittent control models overly rely on keeping each link near a fixed reference position [53]. When confronting complex nonlinear systems with relatively high number of degrees of freedom, such as the triple inverted pendulum, the neural controller is compelled to exhibit characteristics akin to continuous control to maintain the stability of each link. This approach not only loses the natural sway characteristics of the human body but also erroneously shifts the control objective from maintaining the stability of the body's CoM to stabilizing each individual link, which does not align with the actual control mechanisms of human standing [22], [56].

Overall, this study introduces the HTIP model, emphasizing the need to pivot from analyzing the neural control of individual segments to focusing on the neural regulation of the whole body's CoM in neuromechanical modeling of human quiet stance. This approach is also applicable to gait analysis. Given that walking involves multiple segments and joints, including not only the hips, knees, and ankles, but also the shoulders and elbows, modeling each segment's CoM separately leads to substantial complexity [57]. Additionally, this approach necessitates detailed consideration of the neural feedback torques applied to each joint [58]. Concentrating on the global CoM not only simplifies the modeling process but also more accurately reflects the natural control of human motion. Furthermore, state-dependent intermittent control has been employed in several studies to elucidate the control mechanisms governing human gait [59], [60]. Although the HTIP model is not directly translatable to gait research, its foundational concepts are highly applicable and can enrich gait-related studies. This is because, during gait, the CNS manages balance primarily by controlling the overall CoM rather than focusing on the movements of individual body segments, aligning well with the HTIP model's approach.

V. Conclusion

In this study, we introduced a comprehensive neuromechanical modeling approach by integrating a HTIP model with state-dependent intermittent control to simulate human quiet standing. This innovative model combines the computational simplicity of a SIP with the biomechanical complexity of a TIP, capturing the complex dynamic interplay among the ankle, knee, and hip joints in the sagittal plane, and their corresponding segments. Through the application of state-dependent intermittent control, the model mimics natural neural control mechanisms, activating neural feedback based on the stability demands indicated by the motion state of the body's CoM. Our findings demonstrate that the HTIP model, supported by this novel control strategy, successfully replicates natural postural sways observed in human standing, as confirmed by comparisons of simulation results with actual motion capture data. The model's ability to reflect real-time postural adjustments and its adaptability to varying stability conditions were particularly evident in the analysis of angular movements, their power spectral densities, and state phase portraits. The study validates the hypothesis that a hybrid modeling approach in the sagittal plane, coupled with intermittent

control based on the state of the CoM, offers an effective framework for enhancing our understanding of human upright posture control.

Acknowledgment

The authors would like to express their sincere gratitude to Dr. Juzheng Mao from Southeast University, located at No.2 Sipailou, Nanjing, Jiangsu Province, 210096, for his support in providing the experimental facilities and equipment necessary for this research.

Conflict of Interest

The authors declare that the research was conducted in the absence of any commercial or financial relationships that can be construed as a potential conflict of interest.

Ethical Approval and Informed Consent

Ethical approval for this study was obtained from the Imperial College London Research Ethics Committee (Reference: 18IC4685), in compliance with the Declaration of Helsinki. All participants received comprehensive information regarding the study's procedures and potential risks prior to participation, ensuring informed consent was duly obtained. Participation in this study was voluntary, with strict adherence to confidentiality and anonymity. Additionally, support was readily available to address any concerns participants might have following the experiment.

Data Availability Statement

Data will be provided on reasonable request based on ethical, legal or business considerations.

References

[1] D. Gu, K. Andreev, and M. E. Dupre, "Major trends in population growth around the world," *China CDC weekly*, vol. 3, no. 28, p. 604, 2021.

[2] Q. Xu, X. Ou, and J. Li, "The risk of falls among the aging population: A systematic review and meta-analysis," *Frontiers in public health*, vol. 10, p. 902599, 2022.

[3] B. Nordström, A. Näslund, M. Eriksson, L. Nyberg, and L. Ekenberg, "The impact of supported standing on well-being and quality of life," *Physiotherapy Canada*, vol. 65, no. 4, pp. 344–352, 2013.

[4] T. Yamamoto, C. E. Smith, Y. Suzuki, K. Kiyono, T. Tanahashi, S. Sakoda, P. Morasso, and T. Nomura, "Universal and individual characteristics of postural sway during quiet standing in healthy young adults," *Physiological reports*, vol. 3, no. 3, p. e12329, 2015.

[5] F. Quijoux, A. Vienne-Jumeau, F. Bertin-Hugault, M. Lefèvre, P. Zawieja, P.-P. Vidal, and D. Ricard, "Center of pressure characteristics from quiet standing measures to predict the risk of falling in older adults: a protocol for a systematic review and meta-analysis," *Systematic reviews*, vol. 8, pp. 1–9, 2019.

[6] N. Šarabon, Ž. Kozinc, and G. Marković, "Effects of age, sex and task on postural sway during quiet stance," *Gait & Posture*, vol. 92, pp. 60–64, 2022.

[7] G. O'Neill, M. Campbell, T. Matson, and A. Schinkel-Ivy, "How do features of dynamic postural stability change with age during quiet standing, gait, and obstacle crossing?" *Human movement science*, vol. 95, p. 103197, 2024.

[8] Y. Zhao, M. Zhang, H. Wu, X. He, and M. Todoh, "Neuromechanics-based neural feedback controller for planar arm reaching movements," *Bioengineering*, vol. 10, no. 4, p. 436, 2023.

[9] W. H. Gage, D. A. Winter, J. S. Frank, and A. L. Adkin, "Kinematic and kinetic validity of the inverted pendulum model in quiet standing," *Gait & posture*, vol. 19, no. 2, pp. 124–132, 2004.

[10] P. Morasso, A. Cherif, and J. Zenzeri, "Quiet standing: The single inverted pendulum model is not so bad after all," *PloS one*, vol. 14, no. 3, p. e0213870, 2019.

[11] H. K. Abdul-Ameer, "Using a spherical inverted pendulum and statokinesigram for modeling and evaluating quiet standing posture," *Advances in Mechanical Engineering*, vol. 15, no. 8, p. 16878132231190993, 2023.

[12] J. Lee, K. Zhang, and N. Hogan, "Identifying human postural dynamics and control from unperturbed balance," *Journal of NeuroEngineering and Rehabilitation*, vol. 18, pp. 1–15, 2021.

[13] A. Tigrini, F. Verdini, S. Fioretti, and A. Mengarelli, "Center of pressure plausibility for the double-link human stance model under the intermittent control paradigm," *Journal of Biomechanics*, vol. 128, p. 110725, 2021.

[14] J. N. Bartloff, W. L. Ochs, K. M. Nichols, and K. G. Gruben, "Frequency-dependent behavior of paretic and non-paretic leg force during standing post stroke," *Journal of Biomechanics*, vol. 164, p. 111953, 2024.

[15] R. Takahashi, N. Kaneko, H. Yokoyama, A. Sasaki, and K. Nakazawa, "Effects of arousal and valence on center of pressure and ankle muscle activity during quiet standing," *Plos one*, vol. 19, no. 4, p. e0297540, 2024.

[16] Ł. Nowakowski, M. Wysogląd, M. Furmanek, and K. Słomka, "Quantifying intrinsic ankle stiffness in quiet standing: A systematic review," *Journal of Kinesiology and Exercise Sciences*, vol. 33, no. 104, pp. 25–34, 2023.

[17] P. Morasso, "Integrating ankle and hip strategies for the stabilization of upright standing: An intermittent control model," *Frontiers in Computational Neuroscience*, vol. 16, p. 956932, 2022.

[18] M. Günther, S. Grimmer, T. Siebert, and R. Blickhan, "All leg joints contribute to quiet human stance: a mechanical analysis," *Journal of biomechanics*, vol. 42, no. 16, pp. 2739–2746, 2009.

[19] S. Sasagawa, M. Shinya, and K. Nakazawa, "Interjoint dynamic interaction during constrained human quiet standing examined by induced acceleration analysis," *Journal of neurophysiology*, vol. 111, no. 2, pp. 313–322, 2014.

[20] G. Wan, P. Wang, Y. Han, and J. Liang, "Torque modulation mechanism of the knee joint during balance recovery," *Computers in Biology and Medicine*, p. 108492, 2024.

[21] A. Bottaro, M. Casadio, P. G. Morasso, and V. Sanguineti, "Body sway during quiet standing: Is it the residual chattering of an intermittent stabilization process?" *Human movement science*, vol. 24, no. 4, pp. 588–615, 2005.

[22] T. M. Vieira, I. D. Loram, S. Muceli, R. Merletti, and D. Farina, "Recruitment of motor units in the medial gastrocnemius muscle during human quiet standing: is recruitment intermittent? what triggers recruitment?" *Journal of neurophysiology*, vol. 107, no. 2, pp. 666–676, 2012.

[23] J. A. Claassen, D. H. Thijssen, R. B. Panerai, and F. M. Faraci, "Regulation of cerebral blood flow in humans: physiology and clinical implications of autoregulation," *Physiological reviews*, vol. 101, no. 4, pp. 1487–1559, 2021.

[24] D. A. Winter, A. E. Patla, F. Prince, M. Ishac, and K. Gielo-Perczak, "Stiffness control of balance in quiet standing," *Journal of neurophysiology*, vol. 80, no. 3, pp. 1211–1221, 1998.

[25] S. Nema, P. Kowalczyk, and I. Loram, "Complexity and dynamics of switched human balance control during quiet standing," *Biological cybernetics*, vol. 109, pp. 469–478, 2015.

[26] P. A. Forbes, A. Chen, and J.-S. Blouin, "Sensorimotor control of standing balance," *Handbook of clinical neurology*, vol. 159, pp. 61–83, 2018.

[27] J. Schröder, W. Saeys, L. Yperzeele, G. Kwakkel, and S. Truijen, "Time course and mechanisms underlying standing balance recovery early after stroke: design of a prospective cohort study with repeated measurements," *Frontiers in Neurology*, vol. 13, p. 781416, 2022.

[28] M. Zaback, K. J. Missen, A. L. Adkin, R. Chua, J. T. Inglis, and M. G. Carpenter, "Cortical potentials time-locked to discrete postural events during quiet standing are facilitated during postural threat exposure," *The Journal of Physiology*, vol. 601, no. 12, pp. 2473–2492, 2023.

[29] K. Masani, A. H. Vette, and M. R. Popovic, "Controlling balance during quiet standing: proportional and derivative controller generates preceding motor command to body sway position observed in experiments," *Gait & posture*, vol. 23, no. 2, pp. 164–172, 2006.

[30] W.-g. Yao, P. Yu, and C. Essex, "Delayed stochastic differential model for quiet standing," *Physical Review E*, vol. 63, no. 2, p. 021902, 2001.

[31] Y. Li, W. S. Levine, and G. E. Loeb, "A two-joint human posture control model with realistic neural delays," *IEEE Transactions on Neural*

Systems and Rehabilitation Engineering, vol. 20, no. 5, pp. 738–748, 2012.

[32] K. L. McKee and M. C. Neale, "Direct estimation of the parameters of a delayed, intermittent activation feedback model of postural sway during quiet standing," *PLoS One*, vol. 14, no. 9, p. e0222664, 2019.

[33] I. D. Loram, H. Gollee, C. van de Kamp, and P. J. Gawthrop, "Is intermittent control the source of the non-linear oscillatory component (0.2–2hz) in human balance control?" *IEEE Transactions on Biomedical Engineering*, vol. 69, no. 12, pp. 3623–3634, 2022.

[34] P. Gawthrop, I. Loram, and M. Lakie, "Predictive feedback in human simulated pendulum balancing," *Biological cybernetics*, vol. 101, pp. 131–146, 2009.

[35] K. Shen, A. Chemori, and M. Hayashibe, "Human-like balance recovery based on numerical model predictive control strategy," *IEEE Access*, vol. 8, pp. 92 050–92 060, 2020.

[36] D. A. Winter, "Human balance and posture control during standing and walking," *Gait & posture*, vol. 3, no. 4, pp. 193–214, 1995.

[37] P. Gawthrop, I. Loram, H. Gollee, and M. Lakie, "Intermittent control models of human standing: similarities and differences," *Biological cybernetics*, vol. 108, pp. 159–168, 2014.

[38] T. Nomura, Y. Suzuki, and P. G. Morasso, "A model of the intermittent control strategy for stabilizing human quiet stance," *Encyclopedia of Computational Neuroscience*, pp. 1–10, 2020.

[39] K. Iqbal, "Mechanisms and models of postural stability and control," in *2011 annual international conference of the IEEE engineering in medicine and biology society*. IEEE, 2011, pp. 7837–7840.

[40] T. P. Huryn, J.-S. Blouin, E. A. Croft, M. S. Koehle, and H. M. Van der Loos, "Experimental performance evaluation of human balance control models," *IEEE Transactions on Neural Systems and Rehabilitation Engineering*, vol. 22, no. 6, pp. 1115–1127, 2014.

[41] Y. Asai, Y. Tasaka, K. Nomura, T. Nomura, M. Casadio, and P. Morasso, "A model of postural control in quiet standing: robust compensation of delay-induced instability using intermittent activation of feedback control," *PloS one*, vol. 4, no. 7, p. e6169, 2009.

[42] T. Nomura, S. Oshikawa, Y. Suzuki, K. Kiyono, and P. Morasso, "Modeling human postural sway using an intermittent control and hemodynamic perturbations," *Mathematical biosciences*, vol. 245, no. 1, pp. 86–95, 2013.

[43] J. Milton, T. Insperger, and G. Stepan, "Human balance control: Dead zones, intermittency, and micro-chaos," *Mathematical Approaches to Biological Systems: Networks, Oscillations, and Collective Motions*, pp. 1–28, 2015.

[44] A. Rao and H. Palanthandalam-Madapusi, "Event-driven intermittent control in human balancing on an unstable and unrestrained platform," *Journal of Medical and Biological Engineering*, vol. 43, no. 4, pp. 376–385, 2023.

[45] D. A. Winter, A. E. Patla, M. Ishac, and W. H. Gage, "Motor mechanisms of balance during quiet standing," *Journal of electromyography and kinesiology*, vol. 13, no. 1, pp. 49–56, 2003.

[46] S. B. Richmond, B. W. Fling, H. Lee, and D. S. Peterson, "The assessment of center of mass and center of pressure during quiet stance: Current applications and future directions," *Journal of biomechanics*, vol. 123, p. 110485, 2021.

[47] W. T. Edwards, "Effect of joint stiffness on standing stability," *Gait & posture*, vol. 25, no. 3, pp. 432–439, 2007.

[48] M. Günther and H. Wagner, "Dynamics of quiet human stance: computer simulations of a triple inverted pendulum model," *Computer methods in biomechanics and biomedical engineering*, vol. 19, no. 8, pp. 819–834, 2016.

[49] M. P. Kadaba, H. Ramakrishnan, and M. Wootten, "Measurement of lower extremity kinematics during level walking," *Journal of orthopaedic research*, vol. 8, no. 3, pp. 383–392, 1990.

[50] L. M. Nashner, "Analysis of stance posture in humans," in *Motor coordination*. Springer, 1981, pp. 527–565.

[51] Y. Suzuki, H. Morimoto, K. Kiyono, P. G. Morasso, and T. Nomura, "Dynamic determinants of the uncontrolled manifold during human quiet stance," *Frontiers in Human Neuroscience*, vol. 10, p. 618, 2016.

[52] K. Masani, M. R. Popovic, K. Nakazawa, M. Kouzaki, and D. Nozaki, "Importance of body sway velocity information in controlling ankle extensor activities during quiet stance," *Journal of neurophysiology*, vol. 90, no. 6, pp. 3774–3782, 2003.

[53] Y. Suzuki, T. Nomura, M. Casadio, and P. Morasso, "Intermittent control with ankle, hip, and mixed strategies during quiet standing: a theoretical proposal based on a double inverted pendulum model," *Journal of theoretical biology*, vol. 310, pp. 55–79, 2012.

[54] Y. Suzuki, A. Nakamura, M. Milosevic, K. Nomura, T. Tanahashi, T. Endo, S. Sakoda, P. Morasso, and T. Nomura, "Postural instability via a loss of intermittent control in elderly and patients with parkinson's disease: A model-based and data-driven approach," *Chaos: An Interdisciplinary Journal of Nonlinear Science*, vol. 30, no. 11, 2020.

[55] J. J. Koltermann, H. Beck, and M. Beck, "Investigation of the correlation between factors influencing the spectrum of center of pressure measurements using dynamic controlled models of the upright stand and subject measurements," *Applied Sciences*, vol. 10, no. 11, p. 3741, 2020.

[56] Y. Asai, S. Tateyama, and T. Nomura, "Learning an intermittent control strategy for postural balancing using an emg-based human-computer interface," *PLoS One*, vol. 8, no. 5, p. e62956, 2013.

[57] R. Lei, H. David, and K. Laurence, "Computational models to synthesize human walking," *Journal of Bionic Engineering*, vol. 3, no. 3, pp. 127–138, 2006.

[58] K. Shiozawa, J. Lee, M. Russo, D. Sternad, and N. Hogan, "Frequency-dependent force direction elucidates neural control of balance," *Journal of NeuroEngineering and Rehabilitation*, vol. 18, pp. 1–12, 2021.

[59] C. Fu, Y. Suzuki, K. Kiyono, P. Morasso, and T. Nomura, "An intermittent control model of flexible human gait using a stable manifold of saddle-type unstable limit cycle dynamics," *Journal of the Royal Society Interface*, vol. 11, no. 101, p. 20140958, 2014.

[60] C. Fu, Y. Suzuki, P. Morasso, and T. Nomura, "Phase resetting and intermittent control at the edge of stability in a simple biped model generates 1/f-like gait cycle variability," *Biological Cybernetics*, vol. 114, no. 1, pp. 95–111, 2020.